Correlation between the interface structure and magnetic and transport properties for Co/Cu(110) and Ni_8Fe_2/Cu/Co/Cu(110) superlattices

Yoshiaki Saito, Koichiro Inomata, and Keiichiro Yusu
Toshiba Corporation, Advanced Reearch Laboratory, Research and Development Center, Saiwai-ku, Kawasaki 210, Japan

Atsushi Goto and Hiroshi Yasuoka
Institute for Solid State Physics, University of Tokyo, Roppongi, Minato-ku, Tokyo 106, Japan
(Received 6 February 1995; revised manuscript received 8 June 1995)

The correlation between the interface structure and magnetic and transport properties for single-crystal Co/Cu(110) and Ni_8Fe_2/Cu/Co/Cu(110) superlattices has been investigated. The interface structure was changed by changing the argon acceleration voltage of the ion beam sputtering and by annealing the samples. The interface structure was analyzed by simulating the ^{59}Co NMR spectra. NMR is sensitive to the atomic configuration, and as a result, various interface structures (atomic configuration) were obtained, while the other structures remain unchanged. There was a correlation between the atomic configuration and magnetic and transport properties, i.e., the giant magnetoresistance, the magnetization, and the interlayer exchange coupling between the ferromagnetic layers. Both interlayer exchange coupling and magnetization at the interface correlate with the interface structure. The interface structure is important in causing both antiferromagnetic coupling between magnetic layers and a large magnetic moment at the interface, and therefore plays an important role in producing giant magnetoresistance.

I. INTRODUCTION

Various aspects of magnetic multilayers have been investigated by many research groups.[1–8] Some of the major problems to be clarified are the correlation between the magnetic and transport properties and the characterization of the interface structure. Especially, for the giant magnetoresistance (GMR),[3,4] exhibited in many magnetic superlattices, many theoretical[9–14] and experimental[15] studies concluded that a strong spin dependent interfacial scattering plays an important role. But the relationship between the magnetoresistance, magnetization, and interface structure is still far form clear. In this paper we mainly present the relations between GMR, magnetization, and nuclear-magnetic-resonance (NMR) results on (110) single crystal Co/Cu and Ni_8Fe_2/Cu/Co/Cu superlattices, because Co/Cu(110) superlattices showed a large GMR, although Co/Cu(111) superlattices showed a small GMR (40% at 4.2 K).[16] Antiferromagnetic (AF) coupling in Co/Cu(111) superlattices is somewhat unclear, because stacking faults and pinholes may lead to ferromagnetic bridging across neighboring layers, and an enhancement of conduction electron scattering at paramagnetic interfaces[17] and loosely polarized interfacial spins[18] have been proposed as possible mechanisms for creating GMR in Co/Cu(111) superlattices. Up to now, many attempts have been made to reveal the correlation between GMR and interface states for Fe/Cr,[19–21] Co/Cu,[15,22] and NiFe/Cu.[23,24] In many cases, the interfacial structure was investigated by x-ray diffraction because of the easy manipulation. The x-ray diffraction is basically a method to analyze a long-range order of samples, and gives ambiguous information for the lateral scale of interfacial structure, and determination of the lateral length of roughness is difficult.

On the other hand, NMR is sensitive to the atomic configuration, because the hyperfine interaction, B_{hf}, has a substantial contribution from the magnetic moment of the nearest neighbors. Several studies on NMR for Co/Cu superlattices have been already reported.[15,25–30] However, the correlation between the interface structure and the magnetic and transport properties has not been clarified except in our previous paper.[15]

It is important to modify the interfacial structure, keeping the perfect texture of the film, in order to analyze the correlation between the properties of superlattices and the interfacial states. Only superlattices having perfect texture allow the calculation of the interface states. In many studies, interface states have been determined for polycrystalline multilayers, which would not have perfect texture.

From this standpoint, we prepare single-crystal Co/Cu and Ni_8Fe_2/Cu/Co/Cu superlattices, which have (110) texture. The x-ray-diffraction study shows a main diffraction peak at the position of the fcc-Co(220), Ni_8Fe_2(220), and Cu(220) peaks, and first satellite peaks are also observed for all samples. Rocking curve widths for the main peaks are about $1.2\pm0.2°$. This allows us to calculate the interface structure. We tried to modify the interfaces of single-crystal Co/Cu and Ni_8Fe_2/Cu/Co/Cu superlattices by changing the Ar acceleration voltage (V_B) and also annealed Co/Cu superlattices, which had no significant change in x-ray-diffraction pattern below the annealing temperature of 450 °C. As a result, we successfully prepared samples for which the GMR is very different from each other for Co/Cu and

Ni_8Fe_2/Cu/Co/Cu superlattices. Moreover, we have studied the temperature (T) dependence of the interlayer exchange coupling (J) (Ref. 31) minutely for several AF-coupled (Co 10 Å/Cu 10 Å)$_{100}$ superlattices in order to understand better the effect of the J on the interface structure. The T dependence of the saturation field (H_s) or J has been already reported for Co/Cu (Ref. 32) and Fe/Cr (Ref. 33) superlattices. However, the detailed T dependence has not been clarified. For polycrystalline samples, determination of H_s has an ambiguity due to the broad tail of the magnetoresistance (MR) curves and perfect texture is needed for determination of J, because the amplitude of J depends on the films' growth directions. On the other hand, our samples have a high texture and field induced metamagnetic transition due to the large value of the uniaxial anisotropy (K_u) of the order of 10^6 erg/cc,[33,34] so the J can be correctly determined for the [110] direction.

In this work, we show here that there exists a change in interfacial structure which causes a significant change in NMR spectra for Co/Cu and Ni_8Fe_2/Cu/Co/Cu superlattices. For the Ni_8Fe_2/Cu/Co/Cu superlattices, field induced antiparallel magnetic alignment for adjacent magnetic layers separated by Cu layers was observed due to the difference of the coercive force between Co and Ni_8Fe_2 magnetic layers.[35] This allows us to investigate the scattering problem directly. It was revealed that the interface structure at Co/Cu is important in causing both AF coupling between adjacent magnetic layers and a large Co magnetic moment at the interface, and therefore plays an important role in producing the GMR. Moreover, we investigated the T dependence of the J, and found that the amplitude of J is T dependent and has a weak anomaly around $T=30$ K.

II. EXPERIMENT

The single-crystal Co/Cu, Ni_8Fe_2/Cu/Co/Cu superlattices were prepared by ion-beam sputtering (IBS) from Co, Cu, Ni_8Fe_2 targets onto single-crystal MgO(110) substrates at a base pressure of 5×10^{-7} Torr. Sputtering was carried out using 1.6×10^{-4} Torr argon ions. V_B for sputtering was changed from 300 V to 1.4 kV in order to change the randomness at the interface. The substrate temperature was fixed at room temperature in order to conserve other factors except for randomness at the interface. The Co and Cu thicknesses for Co/Cu superlattices were designed at 10 Å and 10 Å, respectively, in which Cu thickness produces the AF coupling between the Co layers separated by the Cu spacer layers, and the Co, Cu, and Ni_8Fe_2 thicknesses were designed at 10, 50, and 20 Å, respectively, for Ni_8Fe_2/Cu/Co/Cu superlattices, in which Cu thickness produces the noncoupling between Co and Ni_8Fe_2 layers. On the top of the (Co 10 Å/Cu 10 Å)$_{100}$ and (Ni_8Fe_2 20 Å/Cu 50 Å/Co 10 Å/Cu 50 Å)$_{10}$ superlattices, 50 Å Cu layers were deposited to prevent oxidation. The amount of Co and Cu was confirmed by chemical analysis using inductively coupled plasma-optical emission spectroscopy with an ambiguity of ±0.5 Å. In addition to the Co/Cu superlattices, Co-Cu (9.5 at. %) alloy films having a thickness of about 1000 Å were also prepared onto single-crystal MgO(110) substrates for comparison. Moreover (Co 10 Å/Cu 10 Å)$_{100}$ superlattices were annealed at temperatures of 150, 300, 450, and 500 °C in a vacuum of 5×10^{-7} Torr, in order to study the changing of the interfaces. The structure of the films was confirmed by x-ray and electron diffractions. Magnetoresistance was measured using a conventional four-point probe method with a magnetic field applied in the plane of films. NMR experiments were performed in zero field using an incoherent spin-echo spectrometer. The ^{59}Co NMR signals in the Co/Cu and Ni_8Fe_2/Cu/Co/Cu superlattices were observed in a wide frequency range from 110 to 230 MHz. In order to calibrate the frequency dependence of the measurement system, the reference signal was measured together with each spin-echo signal. Moreover, we corrected the ω^2 dependence of the spin-echo signal to obtain the number of atoms which resonate at a particular frequency.[36] The magnetic properties for the films were investigated by using a Quantum Design superconducting quantum interference device magnetometer.

III. CALCULATION METHOD OF INTERFACE STRUCTURE

We adopt a simulation method for analyzing the interface structure. This simulation method is useful to recognize the in-plane distribution due to the atomic short-range order (ASRO) parameters, compared with the conventional method using the binomial distribution function,[37] although much time was used to calculate the interface structure. The probability of finding a Co atom at a particular nearest-neighbor Co atom site is given by

$$P(X_i)=X_i+\alpha_i(1-X_i)\ ,$$

where X_i is the average fraction of Co atoms and α_i is the ASRO parameter in the ith layer. $\alpha_i=0$ implies a random distribution of Co and Cu atoms in the ith layer, and $\alpha_i>0$ and $\alpha_i<0$ correspond to the segregation and clustering of the Co and Cu atoms, respectively. We designed the Co thickness at 10 Å for Co/Cu and Ni_8Fe_2/Cu/Co/Cu superlattices. The 10 Å thickness for Co corresponds to eight monolayers of the fcc(110)-oriented plane. Thus the NMR spin-echo intensity for a system having four monolayers of Co and Cu was calculated. The atomic numbers of the system for simulating the atomic configuration, taking ASRO into account, are $20\times20\times6$ for the number of atoms in the directions of the x, y, and z axes, respectively.

First, we give the probability of $P(X_z)=X_z$ to a Co atom at the $(1,1,z)$ coordinate. Then after judging the species of the atoms in the $(1,1,z)$ and $(1,2,z-1)$ coordinates, we give the probability of $P(X_i)=X_i+\alpha_i(1-X_i)$ to the Co atom at the $(1,2,z)$ coordinate. Next, after filling in all the coordinates using this process, we calculate the number of Co atoms for the 12 nearest neighbors. Then we fit the NMR spin-echo intensity corrected by the value of the spin-spin relaxation time with this calculated intensity,[15] taking the boundary conditions of

$(0,i,z)=(20,i,z)$ and $(i,0,z)=(i,20,z)$ $(1\leq i\leq 20)$ into account.

IV. RESULTS AND DISCUSSIONS

A. Structure

Figure 1 shows the transmission electron diffraction (TED) patterns for (Co 10 Å/Cu 10 Å)$_{100}$ and (Ni_8Fe_2 20 Å/Cu 50 Å/Co 10 Å/Cu 50 Å)$_{10}$ superlattices. Only spots of the superlattice and MgO can be observed for all V_B. The structure of Co/Cu and Ni_8Fe_2/Cu/Co/Cu superlattices is perfectly (110) oriented and about 3 vol% distorted face centered cubic (to be exact, face centered tetragonal). In-plane [110] and [100] directions of the Co/Cu and Ni_8Fe_2/Cu/Co/Cu superlattices are parallel to the [110] and [100] directions of the MgO single-crystal substrates, respectively. The x-ray-diffraction study shows a diffraction peak at the position of the fcc-Co(220) and Cu(220) peak for Co/Cu superlattice, and fcc-Co(220), Ni_8Fe_2(220), and Cu(220) peak for Ni_8Fe_2/Cu/Co/Cu superlattices and first satellite peaks were also observed for all samples. Rocking curve widths for the main peaks decrease from 1.37° to 1.13° for Co/Cu superlattices and from 1.63°to 1.35° for Ni_8Fe_2/Cu/Co/Cu superlattices with increasing V_B. Low-angle diffraction peaks due to the superlattice periodicity show only the first-order peak for the 20 Å sum of the Co and Cu layer thickness and show the first- to third-order peaks for the 39 Å sum of the thickness for Co/Cu superlattices and show the second- to fifth-order peaks for Ni_8Fe_2/Cu/Co/Cu superlattices. All samples deposited using different values of V_B have no significant change in x-ray-diffraction pattern except the intensity of the satellite peaks for the mean peaks and low-angle superlattice lines. The intensities of the satellite peaks and low-angle superlattice peaks have a maximum at $V_B=600$ V for Co/Cu superlattices and have a maximum at $V_B=700$ V for Ni_8Fe_2/Cu/Co/Cu superlattices. This intensity behavior correlates with the interface structure as shown in a later section.

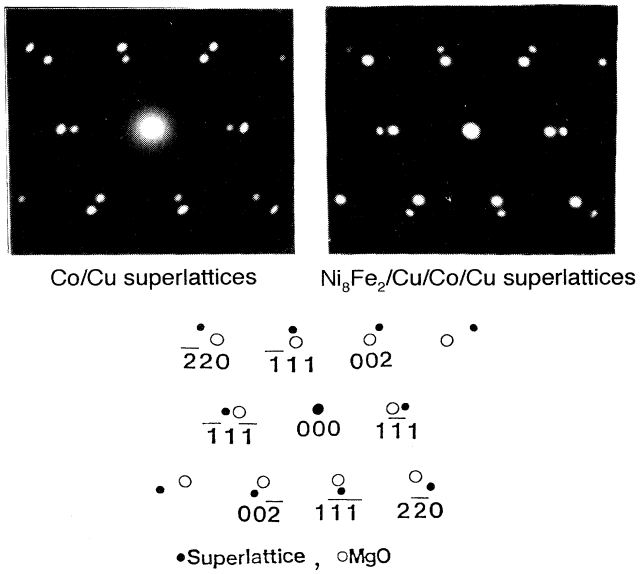

FIG. 1. Transmission electron diffraction patterns for (Co 10 Å/Cu 10 Å)$_{100}$, and (Ni_8Fe_2 20 Å/Cu 50 Å/Co 10 Å/Cu 50 Å)$_{10}$ superlattices.

B. Co/Cu superlattices

Figure 2 shows the V_B dependence of the MR curves at room temperature for (Co 10 Å/Cu 10 Å)$_{100}$ superlattices. The shape of the MR curves is sensitive to V_B. The V_B dependence of the MR ratio is quite strong, and the MR ratio has a maximum around $V_B=700$ V. The field-induced resistivity change ($\Delta\rho$) also has a maximum around $V_B=700$ V, and the saturation resistivity (ρ_s) has a minimum value at $V_B=600$ V.

Figure 3 shows the V_B dependence of the residual magnetization at zero field at room temperature and the saturation magnetization at several temperatures. For the samples with small MR ratios, an increase in the residual magnetization was observed. The residual magnetization

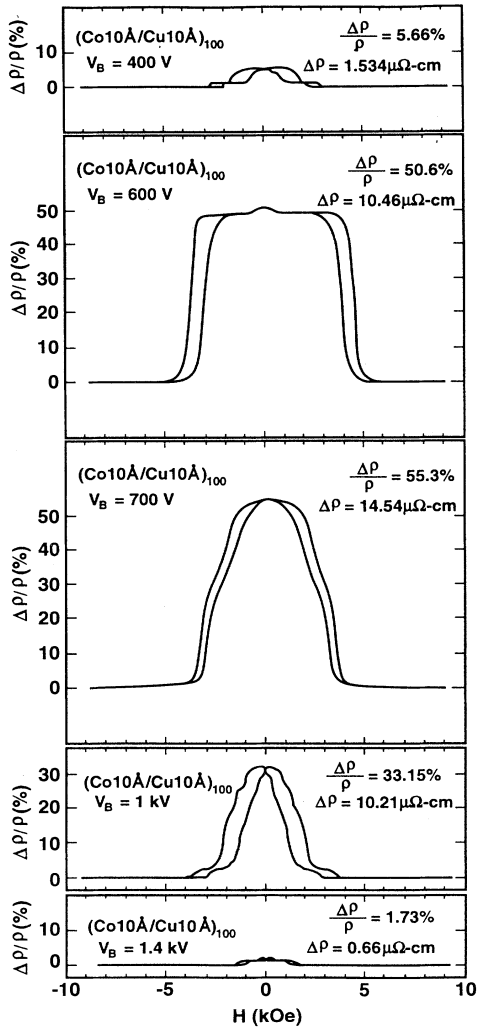

FIG. 2. Argon acceleration voltage dependence of MR curves at room temperature for (Co 10 Å/Cu 10 Å)$_{100}$ superlattices.

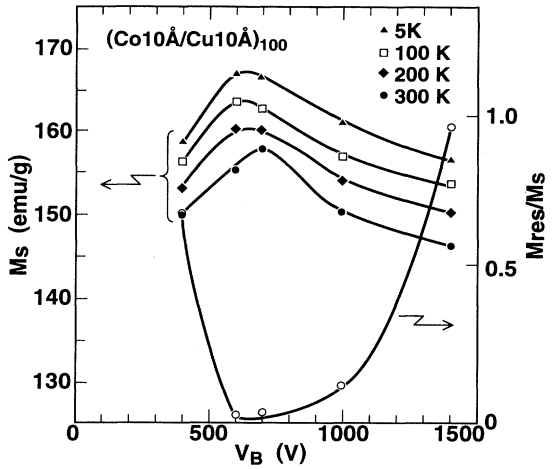

FIG. 3. V_B dependence of the residual magnetization at zero field at room temperature and saturation magnetization at several temperatures for (Co 10 Å/Cu 10 Å)$_{100}$ superlattices.

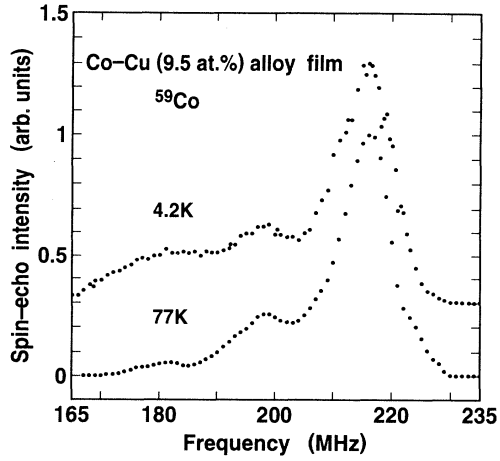

FIG. 4. ^{59}Co NMR spectra of Co-Cu (9.5 at. %) alloy films at 4.2 and 77 K.

is nearly zero and equal between $V_B=600$ and 700 V, although the MR ratio prepared at the condition of $V_B=700$ V is larger than that at $V_B=600$ V. The saturation magnetization (M_s) also has a slight maximum at around $V_B=700$ V at room temperature. This magnetic property is associated with the interface structure in the superlattices, as described later. Interlayer coupling J, uniaxial anisotropy K_u, and saturation magnetization M_s change the shape of the MR curves[38] in accordance with the change in V_B. A K_u of the order of 10^6 erg/cc is introduced with the easy axis of the magnetization parallel to the in-plane Co/Cu[100] direction. This large value of K_u introduces the metamagnetic transition in antiferromagnetically coupled Co/Cu superlattices at the field of $H_s=2J/M_s t$,[38] where t is a ferromagnetic layer thickness (10 Å), when a magnetic field is applied parallel to the easy axis.

In order to analyze the spectra in terms of its local structure, for Co-Cu (9.5 at. %) alloy films, NMR spectra were measured as a reference. The NMR spectra at 4.2 and 77 K for this alloy in zero field are shown in Fig. 4. X-ray-diffraction measurement showed that this film had also a fcc structure with a texture of the [110] direction perpendicular to the film plane. The first and second satellite lines in about 17 and 34 MHz of the lower frequency side, respectively, of the fcc main line (216 MHz) are observed. The resonance frequency of the main line is nearly the same as that of pure fcc Co (217 MHz). The first and second satellite lines are assigned to Co with 11 Co and 1 Cu nearest neighbors and 10 Co and 2 Cu nearest neighbors, respectively. The hyperfine field ($B_{\rm hf}$) of all lines is T independent below 77 K for Co-Cu alloy films.

From these results, the NMR spin-echo intensity of superlattices was analyzed based on the assumption that the substitution of nearest-neighbor Co atoms by Cu atoms yields a discrete shift in $B_{\rm hf}$ due to the reduction of s-electron polarization of Co atoms;

$$B_{\rm hf}=a\mu_{\rm self}+b\sum_i \mu_i \ ,$$

where the first term is the contribution from the self-magnetic moment ($\mu_{\rm self}$) and second term is the contribution from the nearest-neighbor moments (μ_i). Figure 5 shows the NMR spin-echo intensity versus frequency plots in zero field and at 4.2 K for (Co 10 Å/Cu 10 Å)$_{100}$ superlattices prepared at $V_B=400$, 600, 700, 1000, and 1400 V. The lines are widely distributed from 120 to 230 MHz, and the V_B dependence of the NMR spectra is substantial. The main lines in all the spectra in Fig. 5 appear to be close to the value of fcc Co. No signal was observed at the higher frequency side of the fcc line, which indicates that the amount of hcp Co is very small. For a perfectly flat interface, the main line (12 Co nearest neighbors) and two interface lines (11 Co and 1 Cu nearest neighbor, and 7 Co and 5 Cu nearest neighbors) are expected for (110)-textured superlattices. This is not the case for these samples, so the interface regions are rather mixed. The solid lines in Fig. 5 show spectra well fitted by six Gaussian lines, assuming the same value of linewidth for each line. The deviations of the reconstruction of the spectra with six Gaussian lines were very small, as shown in Fig. 5. The spacing between the lines was found to be 15 MHz with a scatter of 2.0 MHz for (110) oriented Co/Cu superlattices.

Figure 6 shows the results of well-fitted parameters of X_i and α_i with an uncertainty of $\pm 10\%$. The form of the interface for Co 10 Å/Cu 10 Å superlattices varies as V_B changes. Alloying mostly occurs within one plane of the interface layer for $V_B=400$ and 600 V, and within two planes for $V_B=700$, 1000, and 1400 V. An important result is the correlation between the MR ratio and X_i. The Co atomic fraction X_i for the interface alloy regions is nearly uniform and equal to 50 at. % for superlattices having small resistivity change ($\Delta\rho$). On the other hand, for superlattices which show large $\Delta\rho$, the tendency of the distribution of X_i in the interface alloy regions from 70 to 30 at. % Co for superlattices prepared under the

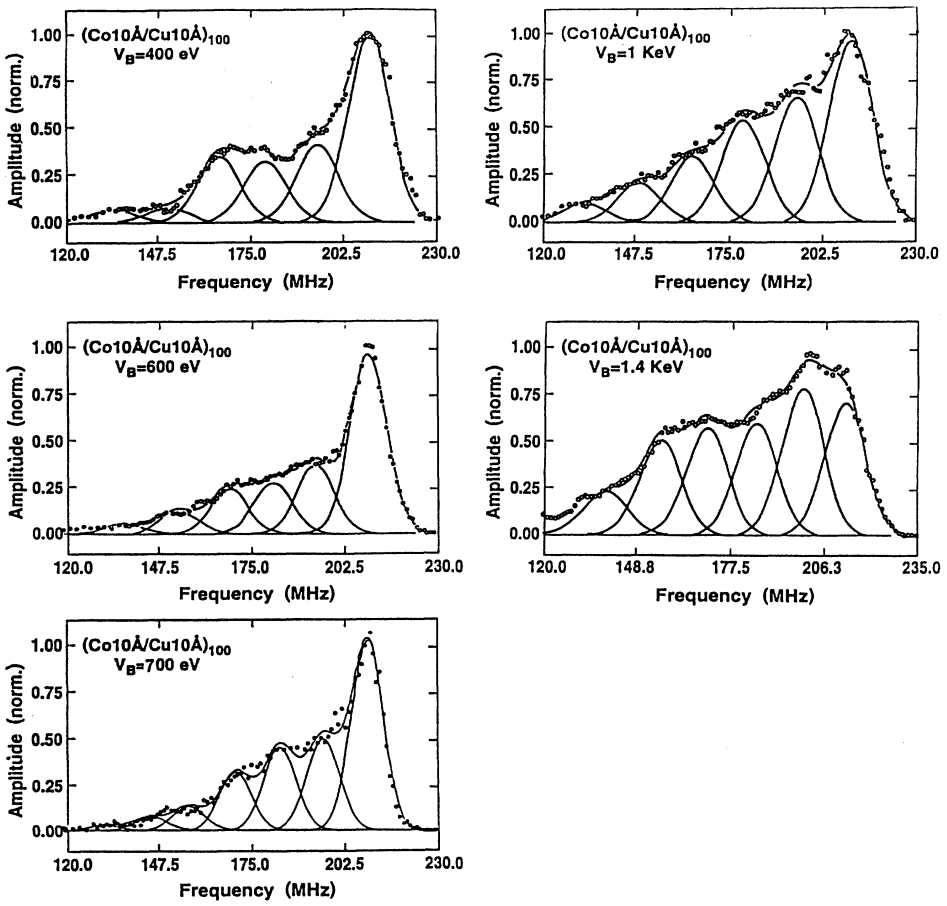

FIG. 5. NMR spectra of (Co 10 Å/Cu 10 Å)$_{100}$ superlattices as a function of V_B. The main line is attributed to fcc Co and the satellite lines to Co at the interfaces of superlattices. Solid lines are fitted results of separated Gaussian lines.

conditions of $V_B = 600$ V, and 95 to 5 at. % Co and 80 to 20 at. % Co for $V_B = 700$ and 1000 V, respectively, is observed. The largest MR ratio was observed at $V_B = 700$ V, which has the interface alloy regions extending over two planes. This suggests that interface structure and GMR are strongly correlated, and that GMR requires atomically mixed interfaces (chemical distribution in the interface alloy region). This chemical distribution changes the magnetic properties as shown in Fig. 3. One is the change of the J between the magnetic layers. The nearly uniform and equal to 50 at. % Co atomic fraction X_i for the interface alloy regions having small MR ratio implies that the number of Cu atoms increases abruptly for 12 Co nearest-neighbor sites at the interface regions. This gives rise to a change in the magnetic properties of Co atoms at the alloy regions so that the amplitude of the AF coupling becomes very weak and magnetic moment for adjacent magnetic layers separated by Cu layers does not show the antiparallel alignment as shown in Table I. Another is the change of the M_s due to the change in the interface magnetization. This would give rise to a change in the scattering of conduction electrons at the interfaces.

The ASRO parameter for the superlattices is between 0 and 0.2. This implies that atoms at the interface are likely to form a random distribution and have a slight tendency to form clusters among the same kind of atoms. This tendency is considered to be due to the immiscible relationship between Co and Cu.

TABLE I. The saturation field and amplitude of the AF coupling estimated from the magnetoresistance data and residual magnetization at zero field at 5 K and room temperature for the several Co/Cu superlattices.

Ar acceleration voltage V_B (V)	H_s (kOe)		$-J$ (erg/cm^2)		M_r/M_s (deg)	
	5 K	297 K	5 K	297 K	5 K	300 K
400	2.07	1.97	0.146	0.140	0.845	0.881
600	5.24	4.22	0.372	0.279	0.019	0.016
700	3.96	3.19	0.280	0.214	0.055	0.052
1k	3.55	2.90	0.252	0.206	0.432	0.378
1.4k	1.25	1.20	0.087	0.085	0.983	0.982

C. Ni_8Fe_2/Cu/Co/Cu superlattices

From the results of the V_B dependence of Co/Cu superlattices, we found that the large MR ratio occurs for a distribution of Co atomic fraction X_i for the interface alloy regions. It was revealed that these interface structures change the magnetic properties such as interlayer coupling and the Co magnetic moment of the interface. The relation between the GMR and the AF coupling has been accepted by many researchers. Therefore we inves-

tigated whether there is a correlation between the MR and the Co magnetic moment at the interface. In order to examine the scattering center problem directly, Ni_8Fe_2/Cu/Co/Cu superlattices are best, because J for this system is nearly zero due to the thick Cu layer, and field induced antiparallel magnetic alignment state between Co and Ni_8Fe_2 layers was observed due to the difference of the coercive force between Co and Ni_8Fe_2.[35] Figure 7 shows magnetization versus magnetic field curves for (Ni_8Fe_2 20 Å/Cu 50 Å/Co 10 Å/Cu 50 Å)$_{10}$ superlattice at 5 K. K_u was introduced due to the epitaxial strain when Co and Ni_8Fe_2 is deposited on Cu as we will describe in Sec. IV E, and the easy axis of the magnetization is the Ni_8Fe_2/Cu/Co/Cu[100] direction. When the field was applied to the Ni_8Fe_2/Cu/Co/Cu[100] direction, field induced antiparallel magnetic alignment states between Co and Cu layer were observed for the all V_B dependence samples.

Figures 8 and 9 show the V_B dependence of the MR ratio and M_s, respectively, for (Ni_8Fe_2 20 Å/Cu 50 Å/Co 10 Å/Cu 50 Å)$_{10}$ superlattices. Large MR ratios were observed associated with the field induced antiparallel magnetic moment state. Both MR and M_s are also sensitive to V_B and have a maximum around $V_B = 700$ V.

Figure 10 shows the ^{59}Co NMR spectra at 1.5 K as a function of V_B for (Ni_8Fe_2 20 Å/Cu 50 Å/Co 10 Å/Cu 50 Å)$_{10}$ superlattices. The lines are widely distributed from 110 to 235 MHz, and the V_B dependence of the NMR spectra is substantial. The main lines in all the spectra in Fig. 10 appear to be close to the value of fcc

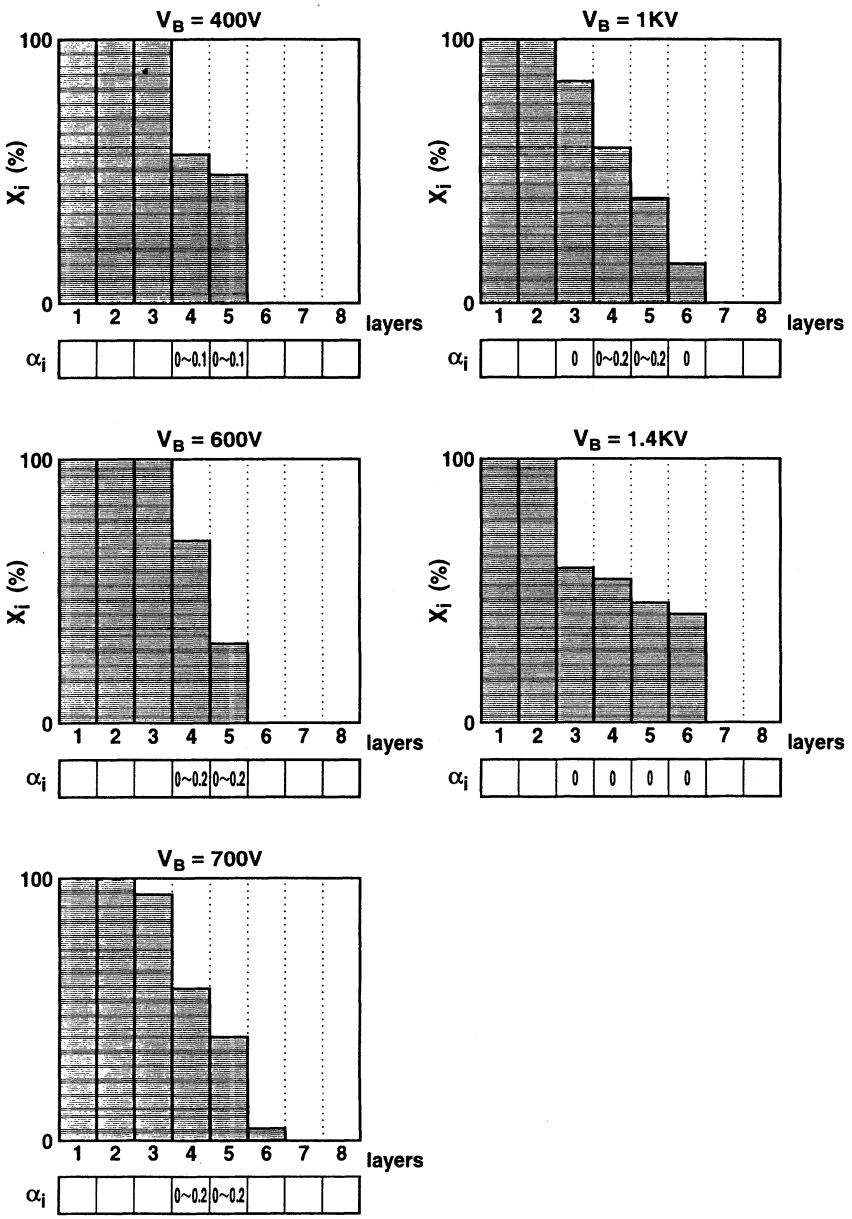

FIG. 6. Calculated average fraction (X_i) for Co and Cu and ASRO parameters (α_i) for superlattices prepared under the conditions of $V_B = 400$ V, 600 V, 700 V, 1 kV, and 1.4 kV for (Co 10 Å/Cu 10 Å)$_{100}$ superlattices.

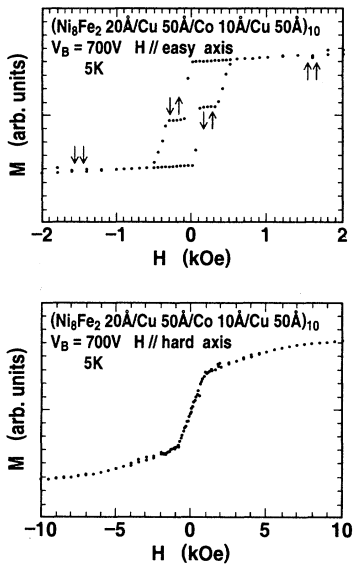

FIG. 7. Magnetization versus magnetic field curves for $(Ni_8Fe_2$ 20 Å/Cu 50 Å/Co 10 Å/Cu 50 Å$)_{10}(110)$ superlattices at 5 K. Uniaxial anisotropy was induced. The easy axis is the Co/Cu/Ni_8Fe_2/Cu[100] direction.

Co. No signal was observed at the higher-frequency side of the fcc line, which indicates that the amount of hcp Co is very small. Also, these samples do not have perfectly flat interfaces. The solid lines in Fig. 10 show spectra well fitted by seven Gaussian lines, assuming the same value of linewidth for each line. The deviations of the reconstruction of the spectra with seven Gaussian lines were very small, as shown in Fig. 10. The spacing between the lines was found to be 15 MHz with a scatter of 2.1 MHz for (110)-oriented Ni_8Fe_2/Cu/Co/Cu superlattices.

Figure 11 shows the results of well-fitted parameters of X_i and α_i. The Co atomic fraction X_i for the interface alloy regions of Co 10 Å/Cu 50 Å varies as V_B changes. Alloying occurs within three planes of the interface layer

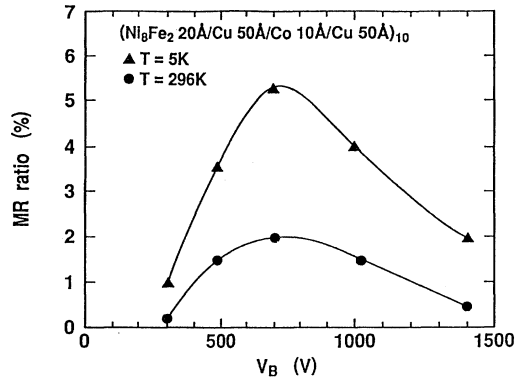

FIG. 8. Argon acceleration dependence of MR ratio at 5 and 296 K for $(Ni_8Fe_2$ 20 Å/Cu 50 Å/Co 10 Å/Cu 50 Å$)_{10}(110)$ superlattices. The field was applied to the easy axis (Co/Cu/Ni_8Fe_2/Cu[100] direction).

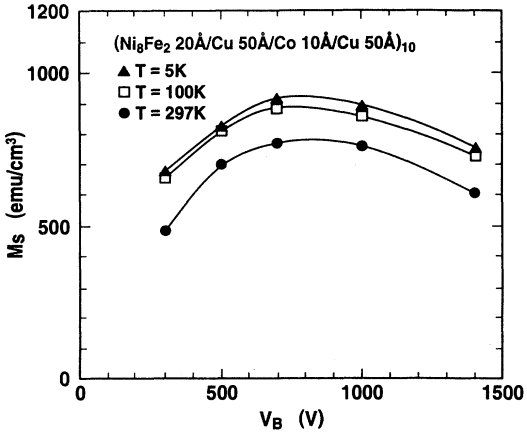

FIG. 9. Argon acceleration dependence of saturation magnetization at 5, 100, and 297 K for $(Ni_8Fe_2$ 20 Å/Cu 50 Å/Co 10 Å/Cu 50 Å$)_{10}(110)$ superlattices.

for all V_B. An important result is the correlation between the MR ratio and X_i. Total numbers of the Co atoms in the mixed Cu interface regions (total numbers of Co atoms in layers 5, 6, and 7 in Fig. 11) for the superlattices having small MR ratio is larger than that for the superlattices having large MR ratio. This suggests that numbers of the Co atoms in the mixed Cu interface and GMR are strongly correlated. Large numbers of the Co atoms in the mixed Cu interface imply the increases in the number of Cu atoms for 12 nearest-neighbor sites to a Co in the interface regions. This may give rise to changes in the magnetic properties of Co atoms at the interface alloy regions so that some spins decrease the magnetic moments due to the hybridization between the Co and Cu atoms. This gives rise to a change in the scattering of conduction electrons.

The ASRO parameter for the Co/Cu interfaces is between 0 and 0.6. This implies that atoms as the interface have a slight tendency to form clusters among the same kind of atoms. This tendency is considered to be due to the immiscible relationship between Co and Cu.

D. Annealing effect for Co/Cu superlattices

Next we study the correlation between the MR ratio and the ASRO parameter, i.e,. segregation of the Co and Cu atoms for Co/Cu(110) superlattices. From the results of the interface structure, the interface alloy regions for the as-deposited (Co 10 Å/Cu 10 Å$)_{100}(110)$ superlattices prepared by the IBS method have an almost random distribution (ASRO parameter $0 \leq \alpha_i \leq 0.2$). We used the annealing method to change the ASRO parameter. Annealing of the Co/Cu superlattices would change the ASRO parameter $\alpha_i > 0$, because Co and Cu atoms have an immiscible relationship. First, we show the annealing temperature (T_A) dependence of the MR ratio for (Co 10 Å/Cu 10 Å$)_{100}$ superlattices. T_A dependence of the MR ratio for the (110) textured (Co 10 Å/Cu 10 Å$)_{100}$ superlattices was not so sensitive below 300 °C as shown in

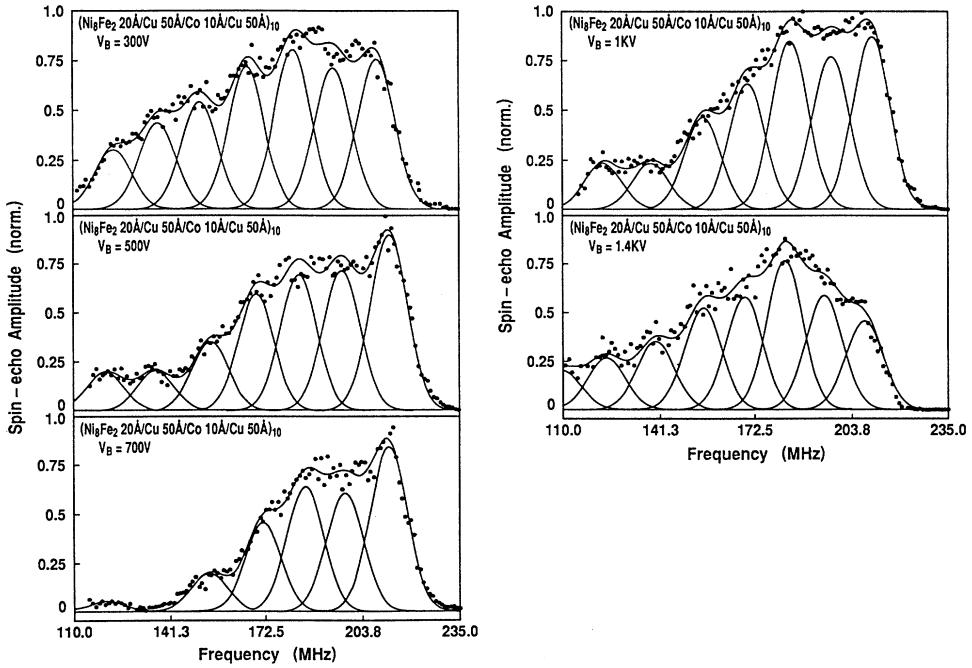

FIG. 10. ^{59}Co NMR spectra of (Ni_8Fe_2 20 Å/Cu 50 Å/Co 10 Å/Cu 50 Å)$_{10}$ superlattices as a function of argon acceleration voltage. Solid curves are fitted results of separated Gaussian lines.

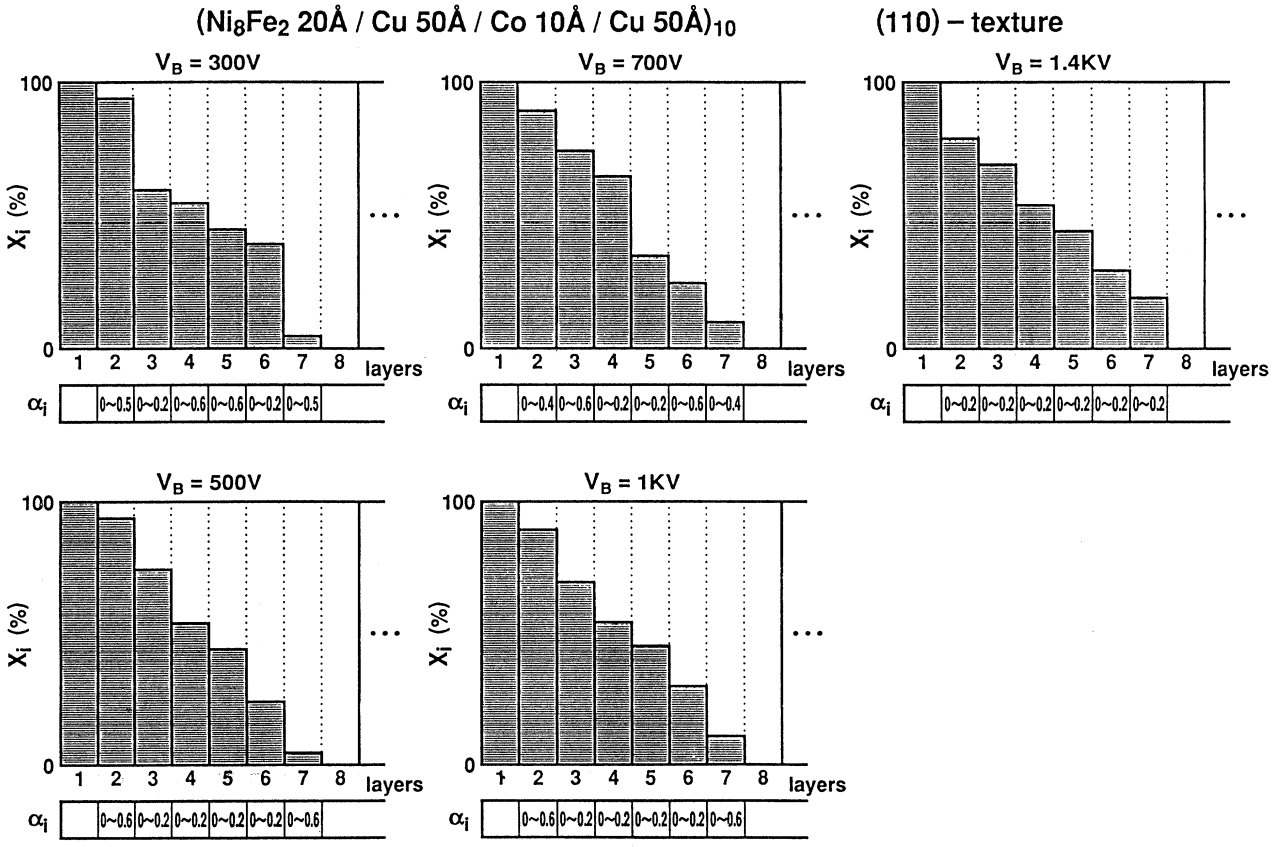

FIG. 11. Calculated average fraction (X_i) for Co and Cu, and ASRO (α_i) parameters for superlattices under the conditions of $V_B = 300$ V, 500 V, 700 V, 1 kV, and 1.4 kV for (Ni_8Fe_2 20 Å/Cu 50 Å/Co 10 Å/Cu 50 Å)$_{10}$ superlattices.

TABLE II. The frequency of the main line of the ^{59}Co NMR spectra for the several Co/Cu and Ni_8Fe_2/Cu/Co/Cu superlattices. The shift in the NMR main line is expressed solely in terms of pure volume lattice expansion. The final entry shows the effect of expanding the Co lattice spacing to match that of Cu lattice.

Sample	$\Delta R/R$(%) at RT	Main line frequency (MHz)	Equivalent lattice expansion $\Delta V/V$(%)
(Co 10 Å/Cu 10 Å)$_{100}$ as deposited	55.3	210.4	2.7
(Co 10 Å/Cu 10 Å)$_{100}$ 150 °C annealing	55.3	210.2	2.8
(Co 10 Å/Cu 10 Å)$_{100}$ 300 °C annealing	55.4	209.0	3.3
(Co 10 Å/Cu 10 Å)$_{100}$ 450 °C annealing	2.1	209.3	3.2
(Co 10 Å/Cu 10 Å)$_{100}$ 500 °C annealing	1.8	216.4	0.23
(Co 25 Å/Cu 10 Å)$_{50}$	33.0	215.0	0.8
(Co 50 Å/Cu 10 Å)$_{40}$	10.5	215.3	0.7
(Ni_8Fe_2 20 Å/Cu 50 Å/ Co 10 Å/Cu 50 Å)$_{10}$ V_B=700 V	2.0	209.0	3.3
Co⟹Cu		204.9	5.3

Table II. When the T_{A_0} was increased to T_A=450 °C, MR ratio for the (Co 10 Å/Cu 10 Å)$_{100}$(110) superlattices became very small, associated with the changing of the J from antiferromagnetic coupling to ferromagnetic (F) coupling. Figure 12 shows the low angle (LA) and high angle (HA) x-ray-diffraction patterns at T_A=150, 300, 450, and 500 °C. Significant change was not observed in x-ray-diffraction measurements below the T_A=450 °C, although the MR ratio fell to a very small value. Only the intensity [half width at half maximum (HWHM)] for the LA x-ray-diffraction patterns slightly decreases (increases) with increasing T_A, although the intensity (HWHM) for the HA x-ray-diffraction patterns increases (decreases) with increasing T_A. When T_A was increased to 500 °C, LA x-ray diffraction disappeared and HA x ray showed the double peaks, whose peak positions are nearly

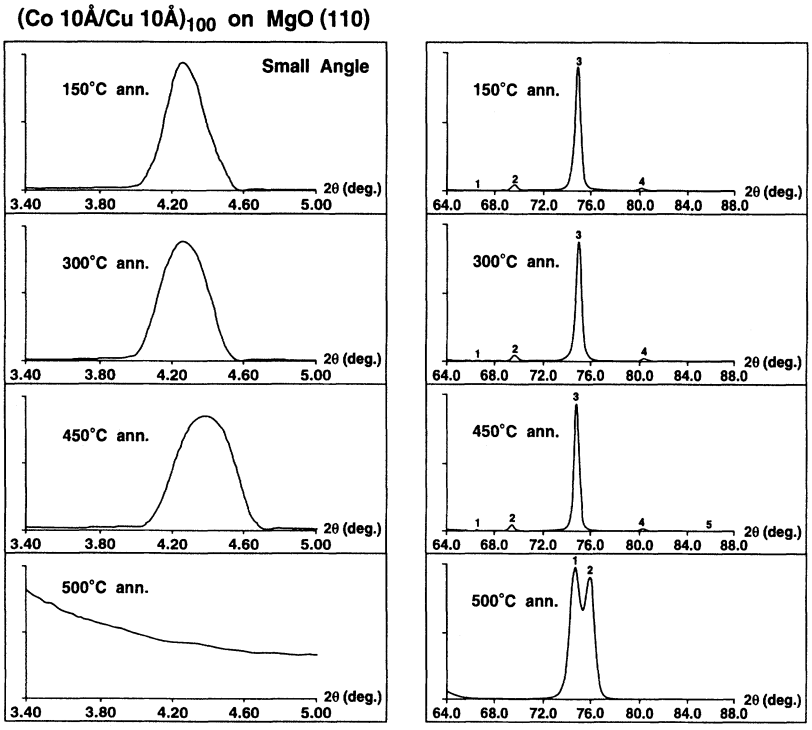

FIG. 12. Low angle and high angle x-ray-diffraction patterns at T_A=150, 300, 450, and 500 °C for (Co 10 Å/Cu 10 Å)$_{100}$(110) superlattices. The x-ray-diffraction pattern of as-deposited (Co 10 Å/Cu 10 Å)$_{100}$(110) superlattices was nearly equal to that of the superlattice annealed at T_A=150 °C.

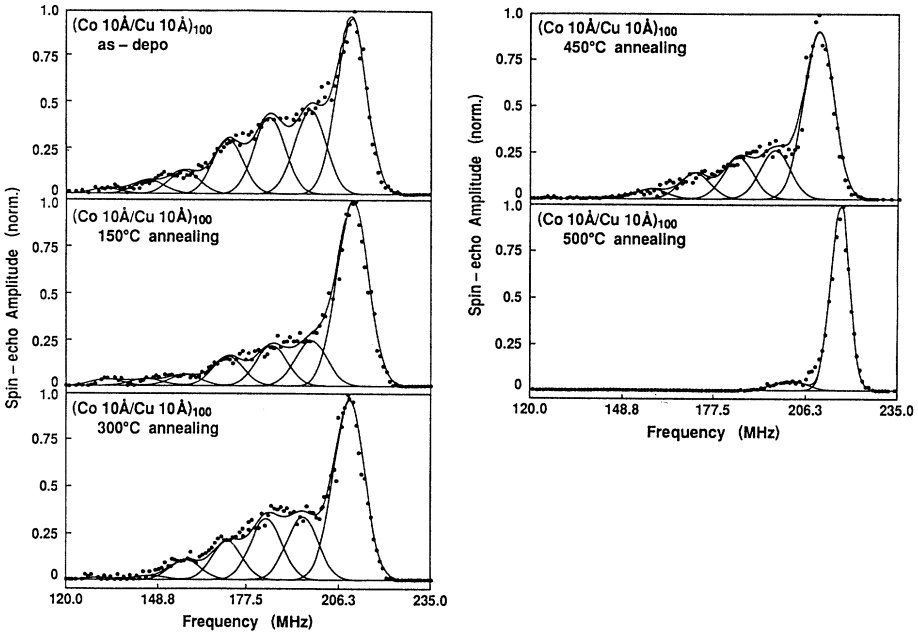

FIG. 13. ^{59}Co NMR spectra for (Co 10 Å/Cu 10 Å)$_{100}$ superlattices as a function of annealing temperature (T_A).

the same at the bulk fcc-Co(220) and Cu(220) positions. A θ scan shows HWHM at 500 °C for HA diffraction patterns becomes smaller than that at 450 °C and is 0.595°, so the degree of the (110) texture is very good for all T_A. Disappearances of the superlattice line in LA x-ray diffraction and satellite lines in HA x-ray diffraction suggest that at $T_A = 500$ °C, diffusion of the atoms is not localized near interfaces and discontinuous states of each layer are realized.

What kind of interface structure is realized for each T_A? Especially, what kind of difference is there between the interface structure at $T_A = 300$ °C and that at 450 °C, which show the differences between MR values, and show the differences between interlayer exchange couplings? Figure 13 shows the ^{59}Co NMR spectra for (Co 10 Å/Cu 10 Å)$_{100}$ superlattices at 4.2 K for various T_A. The lines

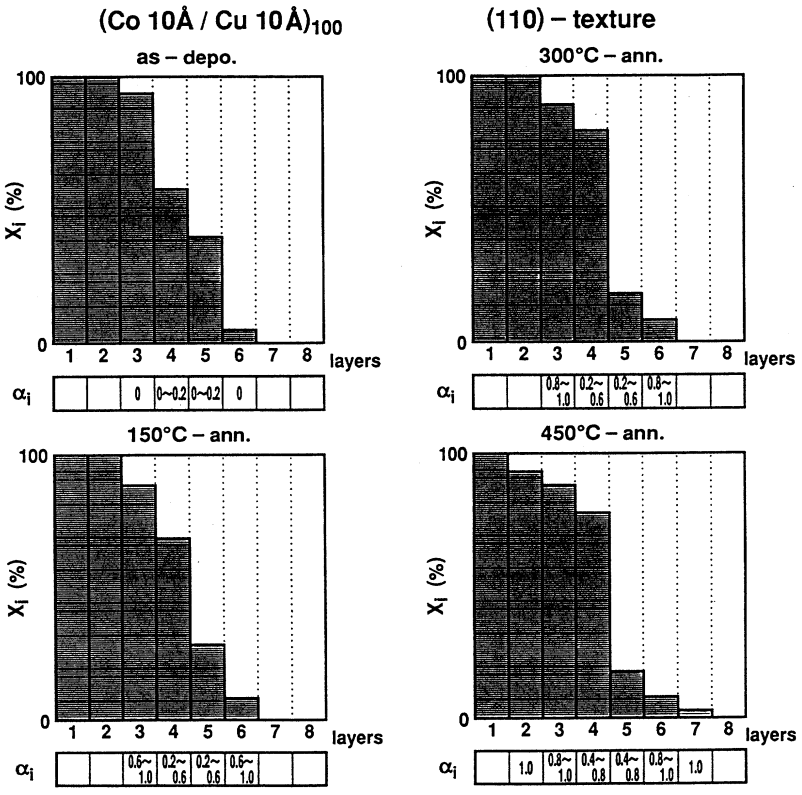

FIG. 14. Calculated average fraction (X_i) for Co and Cu and ASRO parameters (α_i) for superlattices prepared under the conditions of $T_A = 0$, 150, 300, 450, and 500 °C for (Co 10 Å/Cu 10 Å)$_{100}$ superlattices.

for as-deposited Co/Cu superlattices are widely distributed from 120 to 230 MHz and this distribution as a function of the frequency becomes narrower with increasing T_A, and for the superlattices annealed at $T_A=500\,°C$, only the main line and first satellite line were observed. The main lines in the spectra for the samples as deposited and annealed at $T_A=150$, 300, and 450 °C appear to be close to the value of fcc Co or, exactly speaking, exhibited about 7 MHz shifts to the lower frequency side compared with the bulk value, and that for $T_A=500\,°C$ is nearly equal to the value of fcc Co (217 MHz). The hcp-Co line was not observed at the higher frequency side of the fcc line for any T_A. These lines indicate that there is not a perfectly flat (110) interface for any T_A. The solid lines in Fig. 13 are the spectra well fitted by Gaussian lines, assuming the same value of linewidth for each line.

Figure 14 shows the results of well-fitted parameters of X_i and α_i for as-deposited and $T_A=150$, 300, and 450 °C annealed samples. For the sample annealed at $T_A=500\,°C$, we could not simulate the interface structure by approximating it as alloying within three planes of the interface. Interface alloying regions would be more than three planes for the sample annealed at $T_A=500\,°C$. For the samples as-deposited ($V_B=700$ V) and annealed at $T_A=150$ and 300 °C, alloying occurs within two planes of the interface layers and for the sample annealed at $T_A=450\,°C$, alloying occurs within three planes. The ASRO parameter α_i increases with increasing T_A. This is due to the immiscible relationship between Co and Cu. For all samples having interface alloy regions within two planers, both MR ratio and magnetization M_s have nearly the same value, although the values of the ASRO parameter α_i increases. Therefore, increasing of the ASRO parameter α_i does not correlate with the MR ratio. Apparently, increasing of the ASRO parameter α_i shows the segregation of the Co atoms (Cu atoms). For the sample annealed at 450 °C having the interface alloy regions within three planes, in-plane distribution of Co has the island structure (large value of α_i). The interface island structure induces the change of interlayer coupling between magnetic layers from AF coupling to F coupling, the decrease of the MR ratio and the slight increase of M_s ($M_s=162.5$ emu/g at room temperature). From these results, the ASRO parameter α_i are found to not correlate with the MR ratio for the samples having the same interface magnetization.

E. Epitaxial strain and uniaxial anisotropy

It is known that $B_{\rm hf}$ depends on the atomic distance, deduced from its pressure dependence.[39] The pressure has two effects on $B_{\rm hf}$: decrease in the spin density associated with the $3d$ electrons (core contribution), and increase in the magnitude of the valence spin density at the nucleus. For Co, the valence contribution outweighs the core contribution, so a hyperfine field increases its magnitude under pressure. A typical value for Co is $\Delta B_{\rm hf}/B_{\rm hf}=-1.16\Delta V/V$.[39] Thus the shift of the main line of the spectra is related to the atomic volume (V) or the strain in the lattice. Therefore, our result suggests that the Co-Co distance increases when Co is deposited on Cu. The distance between the atoms of Ni_8Fe_2 on Cu also increases because the spot of TED for Ni_8Fe_2/Cu/Co/Cu superlattices shows coherent structure as shown in Fig. 1. As shown in Table II, expansion of the atomic volumes has been estimated from the shifts of the NMR main lines of the several samples. When T_A was increased or Co thickness was increased for Co/Cu superlattices, strain in the Co layers was relaxed. In fact, TED and the x-ray-diffraction studies support this result. This tendency of the strain in the Co layers agrees with the value of K_u. When uniaxial anisotropy is due to this stress induced by epitaxial growth, the elastic energy is written as $K_u=-\sigma\lambda=-(c\varepsilon)\lambda$,[40] where λ is the magnetorestriction constant, ε is epitaxial strain, and c is the elastic tensor. This equation is transformed by $K_u=-c_{11}\lambda_{100}\delta a/a$ when the field is applied to the [100] axis. When c and λ are assumed to have values of the same order as for hcp bulk Co and Ni_8Fe_2, the large value of K_u (5.1×10^6 erg/cc for Co/Cu superlattices and 2.3×10^6 erg/cc for Ni_8Fe_2/Cu/Co/Cu superlattices) can be explained from the order of $\delta a/a=1\%$. This value is nearly the same value as estimated from the TED pattern ($\delta a/a=\sim2\%$ estimated from Fig. 1) and we consider that the large value of K_u is due to the distortion of the lattice. Same behavior was observed for Ni_8Fe_2/Cu superlattices epitaxially grown on a MgO(110) substrates.[40]

F. Amplitude of the interlayer coupling and interface structure

Another important issue is the interlayer exchange coupling (J) between ferromagnetic layers across nonmagnetic spacer layers.[31] Our samples have a metamagnetic transition, so the J can be correctly determined for Co/Cu superlattices having various interface structure using the relation of $H_s=2J/M_st$, when the field is applied to the easy axis direction, where t is thickness of a magnetic layer. Figure 15 shows the typical T depen-

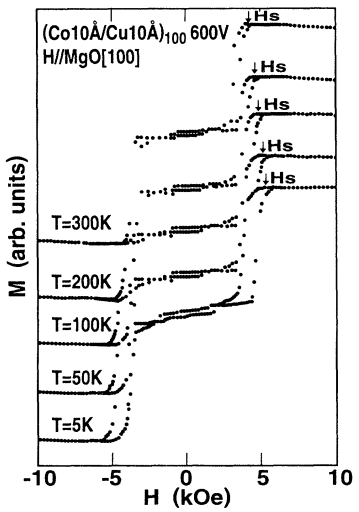

FIG. 15. Magnetization versus field curves at several temperatures for as-deposited (Co 10 Å/Cu 10 Å)$_{100}$ superlattices prepared under the condition of $V_B=600$ V.

dence of the M-H curves for (Co 10 Å/Cu 10 Å)$_{100}$ (V_B=600 V) superlattices. We defined the value of H_s at the middle point of the hysteresis loop of the M-H curves. The H_s is T dependent and increases with decreasing temperature. Figure 16 shows the T dependence of the J for the three (Co 10 Å/Cu 10 Å)$_{100}$ superlattices [V_B=600 V (as deposited), V_B=700 V (as deposited), V_B=700 V (150 °C annealed)]. The amplitude of the J is T dependent and has a weak anomaly around T=30 K. The large T dependence of the J was observed below 30 K, which was suppressed when the sample was annealed at T_A=150 °C. The ^{59}Co NMR spectra for the 150 °C annealed Co/Cu superlattice showed a smaller intensity for the interfacial spin echo spectra than that for the as-deposited Co/Cu superlattice due to the large value of α_i (ASRO parameter) as shown in Fig. 13.

Explanations of the J have been based on the modified Ruderman-Kittel-Kasaya-Yosida theory[41,42] and on the idea of quantum confinement of the electrons within the individual spacer and ferromagnetic layers.[43,44] The observation of oscillations as a function of the ferromagnetic layer thickness in Co/Cu and Fe/Cr multilayers[45,46] is influential and characterized by the quantum confinement theory. Mathon *et al.* showed[44] that T dependence of the J are determined entirely by the properties of the spacer layer Fermi surface (T dependence of the amplitude of J is proportional to $T/\sinh[ak_BT]$, where a is the constant, and k_B is the Boltzmann factor) and independent of the exchange splitting (magnetization) in the ferromagnetic layer, although the overall amplitude of J is determined by two factors: the curvature of the Fermi surface in the nonmagnetic spacer layer and the bulk exchange splitting in the ferromagnetic layers. Our T dependence data of J (a weak anomaly around T=30 K and the large T dependence of the J below 30 K) cannot be explained except for changing the exchange splitting parameter. In order to confirm the effect of the exchange splitting (magnetization in Co) on J, we directly observed the T dependence of B_{hf} at ^{59}Co nucleus for (Co 10 Å/Cu 10.5 Å)$_{100}$ (V_B=700 V) superlattices.[47] The T dependence of the B_{hf} of the interface lines is very large compared with that of the bulk line. This is the evidence that the band state of Co in the interface alloy regions is different from that of bulk Co due to the hybridization of the Co d band with the Cu sp conduction band. This Co band state hybridized with Cu sp conduction band is expected to introduce the effect similar to partial confinement and dependence of the exchange splitting in the ferromagnetic layer. Further work related to the effect of the exchange splitting on J would be necessary.

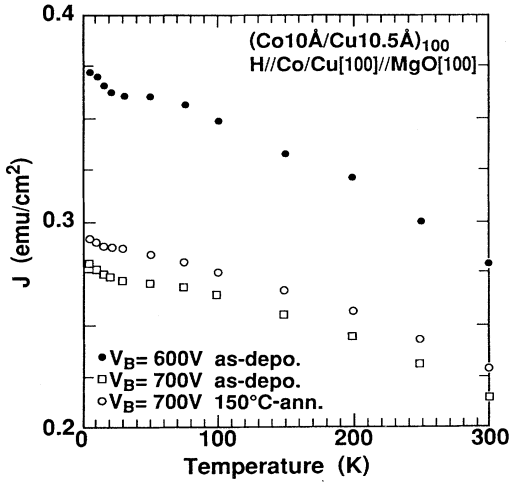

FIG. 16. Temperature dependence of the amplitude of the interlayer exchange coupling between magnetic layers for the three (Co 10 Å/Cu 10 Å)$_{100}$ superlattices under the condition of V_B=600 V (as deposited), V_B=700 V (as deposited), and V_B=700 V (150 °C annealed).

V. CONCLUSION

In conclusion, we studied the correlation between the interface structure, and magnetic and transport properties for Co/Cu(110) and Ni_8Fe_2/Cu/Co/Cu(110) superlattices. As a result, it was found that there is a correlation between interface structure and GMR, M_s, and J. Interface structure causing both AF coupling between magnetic layers and a large magnetic moment at the interface plays an important role in producing GMR. Moreover, we found that the amplitude of J has a weak anomaly around T=30 K.

ACKNOWLEDGMENTS

We gratefully acknowledge assistance with this work by S. Nakamura (Toshiba Corp. R & D Center) for measuring the TED, and by Endo (Toshiba Corp. R & D Center) for measuring the total Co and Cu mass by using the chemical analysis.

[1]P. Grunberg, R. Scheiber, Y. Pang, M. B. Brodsky, and H. Sowers, Phys. Rev. Lett. **57**, 2442 (1986).
[2]P. J. Garcia, A. D. Meinhaldt, and A. Suna, Appl. Phys. Lett. **47**, 178 (1985).
[3]M. N. Baibich, J. M. Broto, A. Fert, F. Nguyen Van Dau, F. Petroff, P. Etienne, G. Creuzet, A. Friederich, and J. Chazelas, Phys. Rev. Lett. **61**, 2472 (1988).
[4]G. Binash, P. Grunberg, F. Saurenbach, and W. Zinn, Phys. Rev. B **39**, 4828 (1989).
[5]D. H. Mosca, F. Petroff, A. Fert, P. A. Schroeder, W. P. Pratt, Jr., R. Laloee, and S. Lequien, J. Magn. Magn. Mater. **94**, L1 (1991).
[6]S. S. P. Parkin, Appl. Phys. Lett. **60**, 512 (1992).
[7]P. J. H. Bloemen, M. T. Johnson, M. T. H. van de Vorst, R. Coehoorn, J. J. de Vries, R. Jungblut, J. aan de Stegge, A. Reinders, and W. J. M. de Jonge, Phys. Rev. Lett. **72**, 764 (1994).
[8]B. Briner and M. Landolt, Phys. Rev. Lett. **73**, 340 (1994).
[9]R. E. Camely and J. Barnas, Phys. Rev. Lett. **63**, 664 (1989).
[10]J. Barnas, A. Fuss, R. E. Camely, P. Grunberg, and W. Zinn, Phys. Rev. B **42**, 8110 (1990).
[11]P. M. Levy, S. Zhang, and A. Fert, Phys. Rev. Lett. **65**, 1643

(1990).
[12]S. Zhang, P. M. Levy, and A. Fert, Phys. Rev. B **45**, 8689 (1990).
[13]J. Inoue, A. Oguri, and S. Maekawa, J. Phys. Soc. Jpn. **60**, 376 (1991).
[14]H. Nakanishi, A. Okiji, and H. Kasai, J. Magn. Magn. Mater. **126**, 451 (1993).
[15]Y. Saito, K. Inomata, A. Goto, and H. Yasuoka, J. Phys. Soc. Jpn. **62**, 1450 (1993).
[16]T. Thomson, P. C. Riedi, and D. Greig, Phys. Rev. B **50**, 10 319 (1994).
[17]D. Bartlett, F. Tsui, D. Glick, L. Lauhon, T. Mandrekar, C. Uher, and R. Clark, Phys. Rev. B **49**, 1521 (1994).
[18]J. C. Slonczewski, J. Appl. Phys. **73**, 5957 (1993).
[19]F. Petroff, A. Barthelemy, A. Hamzi, A. Fert, P. Etienne, S. Lequien, and G. Creuzet, J. Magn. Magn. Mater. **93**, 95 (1991).
[20]E. E. Fullerton, D. M. Kelly, J. Guimpel, I. K. Schuller, and Y. Bruynseraede, Phys. Rev. Lett. **68**, 859 (1992).
[21]P. Blien, R. Schad, C. D. Potter, G. Verbanck, V. V. Moshchalkov, and Y. Bruynseraede, Phys. Rev. B **50**, 9957 (1994).
[22]M. J. Hall, B. J. Hickey, M. A. Howson, C. Hammond, M. J. Walker, D. G. Wright, D. Greig, and N. Wiser, J. Phys. Condens. Matter **4**, L495 (1992).
[23]T. C. Huang, J. P. Nozieres, V. S. Speriosu, H. Lefakis, and B. A. Gurney, Appl. Phys. Lett. **60**, 1573 (1992).
[24]V. S. Speriosu, J. P. Nozieres, B. A. Gurney, B. Dieny, T. C. Huang, and H. Lefakis, Phys. Rev. B **47**, 11 579 (1993).
[25]K. Le Dang, P. Veillet, H. He, F. J. Lamelas, C. H. Lee, and R. Clarke, Phys. Rev. B **41**, 12 902 (1990).
[26]H. A. M. de Gronckel, K. Kopinga, W. J. M. de Jonge, P. Panissod, J. P. Schille, and F. J. A. den Broeder, Phys. Rev. B **44**, 9100 (1991).
[27]C. Meny, P. Panissod, and R. Loloee, Phys. Rev. B **45**, 12 269 (1992).
[28]Y. Suzuki, T. Katayama, and H. Yasuoka, J. Magn. Magn. Mater. **104**, 1843 (1992).
[29]J. S. Lord, H. Kubo, P. C. Riedi, and H. H. Walker, J. Appl. Phys. **73**, 6381 (1993).
[30]M. Suzuki, Y. Taga, A. Goto, and H. Yasuoka, J. Magn. Magn. Mater. **126**, 495 (1993).
[31]S. S. P. Parkin, N. More, and K. P. Roche, Phys. Rev. Lett. **64**, 2301 (1990).
[32]S. S. P. Parkin, R. Bhadra, and K. P. Roche, Phys. Rev. Lett. **66**, 2152 (1991).
[33]M. From, L. X. Liao, J. F. Cochran, and B. Heinrich, J. Appl. Phys. **75**, 6181 (1994).
[34]Y. Saito, H. Hashimoto, and K. Inomata, IEEE Trans. Magn. **28**, 2751 (1992).
[35]T. Shinjo and H. Yamamoto, J. Phys. Soc. Jpn. **59**, 3061 (1990).
[36]H. Yasuoka, in *Metallic Superlattices,* edited by T. Shinjo and T. Takada (Elsevier, Amsterdam, 1987), p. 159.
[37]N. Hamada, K. Terakura, K. Takanashi, and H. Yasuoka, J. Phys. F. **22**, 1057 (1974).
[38]K. Inomata and Y. Saito, Appl. Phys. Lett. **61**, 726 (1992).
[39]J. F. Jank, Phys. Rev. B **21**, 2206 (1979).
[40]K. Inomata and S. Hashimoto, J. Appl. Phys. **74**, 40 (1993).
[41]R. Coehoon, Phys. Rev. B **44**, 9331 (1991); C. Chappert and J. P. Renard, Europhys. Lett. **15**, 533 (1991); D. M. Deaven, D. S. Rokhsar, and M. Johnson, Phys. Rev. B **44**, 5977 (1991).
[42]P. Bruno and C. Chappert, Phys. Rev. Lett. **67**, 1602 (1991); Phys. Rev. B **46**, 261 (1992).
[43]D. M. Edwards, J. Mathon, R. B. Muniz, and M. S. Phan, Phys. Rev. Lett. **67**, 493 (1991); J. Phys. Condens. Matter **3**, 4941 (1991).
[44]J. Mathon, M. T. Johnson, M. T. H. van de Vorst, R. Coehoon, and J. J. de Jonge, Phys. Rev. Lett. **72**, 764 (1994).
[45]P. J. H. Bloemen, M. T. Johnson, M. T. H. van de Vorst, R. Coehoon, J. J. de Vries, R. Jungblut, J. aan de Stegge, A. Reinders, and W. J. M. de Jonge, Phys. Rev. Lett. **72**, 764 (1994).
[46]S. N. Okuno and K. Inomata, Phys. Rev. Lett. **72**, 1553 (1994).
[47]Y. Saito, K. Inomata, A. Goto, H. Yasuoka, S. Uji, T. Terashima, and H. Aoki, Phys. Rev. B **51**, 3930 (1995).

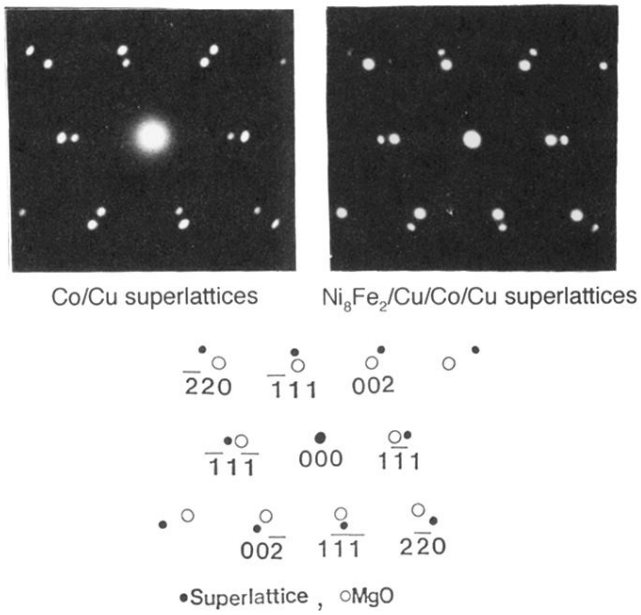

FIG. 1. Transmission electron diffraction patterns for (Co 10 Å/Cu 10 Å)$_{100}$, and (Ni_8Fe_2 20 Å/Cu 50 Å/Co 10 Å/Cu 50 Å)$_{10}$ superlattices.